NUMERICAL STUDIES ON HIGH LIFT GENERATING AEROFOILS TO BE USED AS AIRCRAFT FUSELAGE

Rajan J. Bhatt [1*], Sandip C.Patel[2*], K.Raja Shekar Rao[2*], Dr. S.A. Channiwala [3*]

1. Ph.D student of SVNIT, Surat
2. M.Tech student of SVNIT, Surat
3. Professor of SVNIT, Surat

Abstract

The aerofoil sections investigated in this study are the ones which can be deployed in the high-lift Technology Concept Fuselage in Airplanes . This work is directed towards attainment of substantially higher lift coefficients, needed for future generations of quiet transport aircraft with short take-off and landing capabilities (STOL). The data are obtained with CFD technique for AOA from to 12 for standard high lift generating airfoils viz; Gottingen 398, NACA 4415 and Gottingen 535 and the results were compared with published data of C_L and C_D for these airfoils. An aerofoil section (HLFAirfoil) specially developed for deployment as aircraft fuselage has also been evaluated using the numerical method and the results have been compared with the data of available high lift generating sections. Much better C_L values with reduced C_D values without any flow separation upto AOA of 12 degrees as compared to available high lift generating sections clearly establishes the superiority of proposed HLF airfoil section to be used as fuselage to achieve STOL capabilities for airplane.

Keywords : CFD, High Lift Airfoils, Fuselage.

INTRODUCTION

The present investigation was undertaken in connection with the High Speed Research (HSR) Program, which is investigating the potential benefits and trade-offs of advancements in aerodynamic efficiency, structures and materials, propulsion systems, and stability and control requirements applied to advanced subsonic as well as supersonic cruise aircraft concepts. The configuration investigated in this study is the Technology Concept Airplane fuselage. During takeoff and landing, due to high angle of attack the flow separates from the leading edge of the wing and a vertical flow field develops on the upper surface of the wing; this causes an increase in drag. To establish airports close to city centres, runway lengths have to be reduced to a minimum, thus Short Take-Off and Landing (STOL) performance of the aircraft becomes mandatory. As a requirement to be met under all circumstances, the operation has to comply with or even surpass today's safety standards. The STOL capabilities as a prerequisite for minimum runway lengths can only be achieved by pursuing innovative high-lift concepts even if extreme lightweight airframe materials and structures are used. [1]

One of the most important needs in the aerospace industry is to be able to use CFD to predict a priori scale effects and configuration effects in wing design. Currently, most wind tunnels operate at lower-than-flight Reynolds numbers, and scale effects are poorly understood. Therefore, use of wind tunnel data alone to design a wing can introduce a significant amount of uncertainty.

A review of present CFD capability was carried out for prediction of high lift [2]. A survey was conducted of CFD methods applied to the computation of high-lift multi-element configurations over the last 10–15 years. Both 2-D and 3-D configurations were covered. The review was organized by configuration, in an effort to gain useful insights with respect to particular successes or failings of CFD methods as a whole. In general, for both 2-D and 3-D flows, if certain guidelines regarding grid, transition, and turbulence model are followed, then surface pressures, skin friction, lift, and drag can be predicted with reasonably good accuracy at angles of attack below stall. Velocity profiles can generally be predicted in 2-D flow fields, with the exception of the slat wake, which tends to be predicted too deep by most CFD codes for a range of different configurations. On the whole, 2-D CFD is unreliable for predicting stall (maximum lift and the angle of attack at which it occurs); in most cases, maximum lift was over predicted, but for some configurations the opposite occurs. However, there was some evidence that stall mis prediction of nominally 2-D experiments may be caused by 3-D effects, which were obviously not modelled by 2-D CFD. In general, 3-D computations were also inconsistent with respect to computing stall, but there have been fewer of

these applications to date. The paper concludes with a list of challenges that confront CFD at the start of the next decade, which should witness a dramatic increase in the number of CFD applications for 3-D high-lift configurations.

The Analysis of Post-Support and Wind-Tunnel wall interference on Flow Field about Subsonic High-Lift High-Speed Research Configuration, Experimental forces, moments, and surface pressures are compared with computational data was studied by T. J. Mueller [3]. The results of the wing-body TCA high-lift configuration in free air and with post wind-tunnel walls are presented.

Nathan Logsdon , Dr. Gray Solbrekken[4] have developed a procedure to model airflow numerically over airfoils using Gambit and FLUENT. They created and meshed two and three dimensional models for the airfoil 0012 in Gambit using geometry. Data for airfoil geometry was collected from the National Advisory Committee for Aeronautics. Those models were read into FLUENT where flow boundary conditions were applied and the discretized Navier-Stokes equation were solved numerically.
The airfoil sections lift coefficient from the numeric simulation as compared with experimental data from the literature and shown to agree within 10% for angle of attack below 10^0. Accurate lift coefficients could not be generated for angles of attack greater than 10^0. They made an attempt to demonstrate wing tip vortices from the 3-D model. Unfortunately , due to the inability to develop a reliable mesh this task was not successfully completed. As the angle of attack increased the accuracy of both models dropped dramatically.

F. X. Wortmann [5] studied the aircrafts that fly in a low Reynolds number range which is much less explored. He stated that the requirements with respect to suitable aerofoil for the wing in these aircrafts are much simpler since these machines are aimed to fly mostly between the best glide ratio and the stalling speed. He concluded that at the high aspect ratio of wings, the aerofoils will develop minimum drag when C_L value is between 1.0 t0 1.4 and Reynolds number is between $3x10^5$.
F. Le Chuiton et al. [6] have made the computation of the Helicopter Fuselage Wake with the SST, Model. Results for the loads, pressure distribution and skin friction lines have been compared to each other and against wind tunnel experimental data with flow angle of side-slip $\beta = 0^0$, Mach number $M\infty = 0.116$ and Reynolds number per unit length $Re = 2.5x10^6$. As expected all simulations capture equally well the pressure distribution on the top centre-line, apart from the tail boom where both the XLES and the DES computations, in accordance to each other, predict a somewhat lower pressure. On the bottom symmetry line, the front part doesn't raise any problem either, but discrepancies between the various solutions occur in the region of the backdoor. Almost all simulations render correctly the pressure rise on the top part of the backdoor close to the junction to the tail boom. On the opposite, close to the support strut, the agreement could be better: all but the XLES simulation overestimate the pressure, while the XLES underestimates it.

S. Melber-Wilkending et al. [7] have used the MEGAFLOW-Software for High Lift Applications. This project is concerned with the numerical simulation of the viscous compressible flow around transport aircraft high lift configurations and its validation against wind tunnel experiments. The investigations are based on the solution of the Reynolds-averaged Navier-Stokes equations (RANS) using the MEGAFLOW code system with a finite volume parallel solution algorithm. The numerical simulation of the flow around a complete aircraft in high lift configuration up to maximum lift conditions is one of the major areas. The reference experiments are conducted in the large low speed facility of the German-Dutch wind tunnel DNW at a free stream Mach-number of $M = 0.22$ and a chord Reynolds number of $Re = 2x10^6$. In this numerical analysis angle of attack $\alpha < 15^\circ$ is quite good, the predicted lift coefficients between $15^\circ < \alpha < 22^\circ$ are 5% lower than the measured coefficients. Beginning with $\alpha = 22^\circ$ the lift increases again, without predicting a clear maximum lift in the simulated range angle of attack. For a descriptive discussion of the lift breakdown, the subsequent section includes flow-field stream-line figures at angles of attack of 4°, 12° and 22°.
Christopher L. Rumsey. [8] have given an overview of CFD capability applied to the prediction of high-lift flow fields. A survey is conducted of CFD methods applied to the computation of high-lift multi-element. In general, for both 2-D and 3-D flows, if certain guidelines regarding grid, transition, and turbulence model are followed, then surface pressures, skin friction, lift, and drag can be predicted with reasonably good accuracy at angles of attack below stall. Velocity profiles can generally be predicted in 2-D flow fields, with the exception of the slat wake.

In general the study of literature reveals that the CFD predictions are reliable near cruise conditions where there is little or no flow separation and other high lift devices are not deployed.

2.1 CFD ANALYSIS OF AEROFOIL IN 2D

The central theme of this research project is to do the aerodynamic design of the fuselage of an aircraft, such that it results in generation of extra lift for the aircraft, along with simultaneous reduction of drag, thereby not only reducing the takeoff and landing velocities of the aircraft but also, significantly reducing their propulsive thrust requirement. This proposition has far reaching consequences not only in terms of improved economy and reduced emissions, but also enhanced safety of operation. Towards this end the initial calculations and estimations were done by obtaining the technical data of three of the most commonly used passenger aircrafts viz, Boeing 747, Airbus A310, and Boeing 777. The modified fuselage shapes were based on some of the standard published NASA aerofoils, and using the available data, the implications of the modified fuselage shape were evaluated.

Initially NACA's Gottingen 398 aerofoil was chosen to represent the aircraft fuselage. The reason for this choice was that the foil is geometrically very similar to the special aerofoil designed for this purpose and its performance parameters are available from NACA's published data. Using this aerofoil the CFD analysis was carried out and C_L, C_d and C_M coefficients were evaluated for various angles of attack with 50 m/sec air velocity. This air velocity was chosen for CFD analysis purpose due to the fact that the whole objective of this research is to evolve a fuselage which will generate additional lift thereby bringing down the takeoff velocity from the present magnitude of around 300kmph to a value in between 150 to 200kmph which translates to about 45 to 55m/s. The CFD analysis was carried out using fluent software. The results were subsequently compared with published data. Later two more aerofoils from NACA series viz: NACA 4412 and Gottingen 535 were tested in similar fashion and the CFD capabilities were ascertained through its validation with published data.
In the subsequent stage a more focused attempt was done to develop a dedicated aerofoil shape to serve as the fuselage of a midsized commercial aircraft. Various aerofoil shaped designs were considered, not only from aerodynamics point of view but also the economics and the architectural point of view. These shapes were tested for their aerodynamic characteristics using standard available design software, as well as CFD. Highest lift and lowest drag coefficients at operating conditions were sought at the same time, while keeping an eye on the availability of the cubical volume within the boundaries of the aerofoil section so as to allow accommodation of the requisite number of passengers, cargo, amenities and flight deck. CFD analysis of this specially developed airfoil was carried out in the similar way and finally a comparative assessment of all four high lift generating airfoils is made and conclusions are drawn from it.
To perform the numerical analysis the flow field around the airfoil was modelled using GAMBIT software. While doing the meshing the following criteria were kept in mind.

I. The nodal points near the airfoil are closely clustered since this is where the flow is modified the most; the mesh resolution becomes progressively coarser as the far field boundaries are approached since the flow gradients in this area approaches zero.
II. Close to the surface maximum resolution is needed near the leading and trailing edges since these are critical areas with the steepest gradients.
III. Transitions in mesh size should be smooth; large, discontinuous changes in the mesh size significantly decrease the numerical accuracy.

The meshed model was read into fluent for numerical iterative analysis. The following parameters were employed for processing.

- Solver : Pressure based solver
- Medium : Air (ρ= 1.2256 kg/m3, μ= 1.789 e-5 kg/m-s)
- Viscous Model : Laminar
- Operating Conditions: Pressure=101325pa, Temperature=300 ^{0}K
- Boundary Conditions: Velocity Inlet, Pressure Outlet.
- Solution Controls: Pressure Velocity Coupling - SIMPLE
- Pressure Discretization : PRESTO
- Momentum: Second Order Upwind Scheme
- Initialization : Inlet Values
- Force Monitors : Lift and Drag
- Reference Values : Inlet Values
- Convergence Limit : $1x10^{-6}$

3. RESULTS AND DISCUSSION

The results of the CFD are graphically displayed through Pressure and Velocity Contours and pressure coefficient profile which are shown for each airfoil examined. The comparison of the data arrived at by the CFD approach and that published by NACA which is largely based on their extensive experimental work for the three standard aerofoils is given in the tabular form for each airfoil.

GOTTINGEN 398

Gottingen 398 is one of the earliest and most used airfoil for aircraft applications especially because of the high lift it generates. It is relatively thicker and has been deployed on many civilian and military aircrafts.

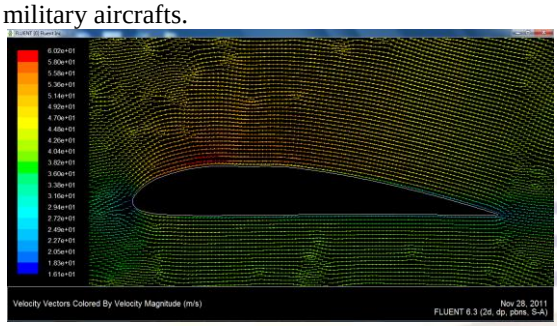

Fig 1: Velocity contours around Gottingen 398 Airfoil at AOA=0^0

Figure 1 shows the velocity contours that develop around the Gottingen 398 foil. As can be seen the velocities over the hump portion of the airfoil exceed those at the lower surface by a factor of about 1.5.

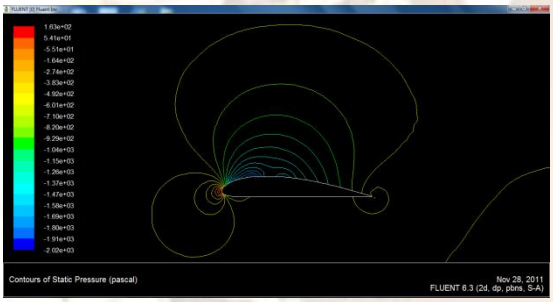

Fig 2: Pressure contours around Gottingen 398 Airfoil at AOA=0^0

Figure 2 depicts the pressure contours enveloping the Gottingen 398 airfoil. The low pressure areas above the hump coincide with the high velocity areas observed in figure 1.

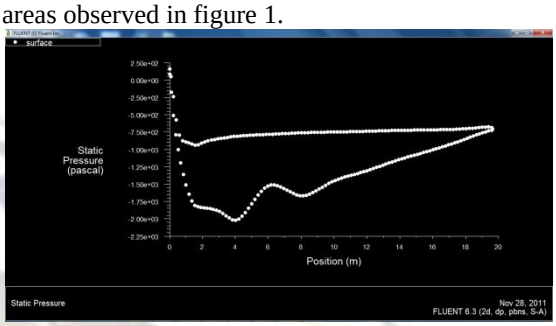

Fig 3: Pressure Coefficient along the chord line for Gottingen 398 Airfoil at AOA=0^0

Figure 3 shows the chord wise pressure distribution over the upper and lower surfaces of the Gottingen 398 airfoil. The upper curve corresponds to the pressure distribution on the lower surface and vice versa.

Force vector: (1 0 0)

zone name	pressure force n	viscous force n	total force n	pressure coefficient	viscous coefficient	total coefficient
surface	454.41926	91.290943	545.7102	0.021820491	0.004383646	0.026204137
net	454.41926	91.290943	545.7102	0.021820491	0.004383646	0.026204137

Force vector: (0 1 0)

zone name	pressure force n	viscous force n	total force n	pressure coefficient	viscous coefficient	total coefficient
surface	12078.427	0.47277906	12078.9	0.57998686	2.2702099e-05	0.58000956
net	12078.427	0.47277906	12078.9	0.57998686	2.2702099e-05	0.58000956

Table 1: Force reports of Gottingen 398 Airfoil at AOA=2^0

ANGLE OF ATTACK	CFD DATA		PUBLISHED DATA		DIFF. CFD & PUBLISHED DATA	
	C_L	C_d	C_L	C_d	C_L	C_d
0	0.450	0.015	0.42	0.02	+7.1%	-25.0%
2	0.589	0.027	0.55	0.03	+7.0%	-10.3%
4	0.759	0.034	0.74	0.04	+2.0 %	-15.0%
6	0 .916	0.048	0.88	0.06	+4.0%	-20.0%
8	1.102	0.055	1.02	0.08	+8.0%	- 31.0%
10	1.248	0.068	1.15	0.1	+8.5%	-32.0%

12	1.398	0 .088	1.26	0.12	+10.9%	-26.7%
14	1.452	0.112	1.4	0.14	+3.7%	-20.0%

Table: 2. Comparison of CFD data with NACA's published data for Gottingen 398 aerofoil

Table 1 shown above is the force report generated by fluent software for Gottingen 398 airfoil at 2 degrees AOA. Force vector (1,0,0) corresponds to the drag force experienced by the airfoil where as the vector (0,1,0) depicts the value of lift.

Table 2 shows the compilation of lift and drag coefficients generated as above for all the values of angle of attack considered and also gives a comparative picture of those values with published data of the agency.

NACA 4415

NACA 4415 is also a high lift generating airfoil which has been extensively used for helicopters and wind turbine applications.

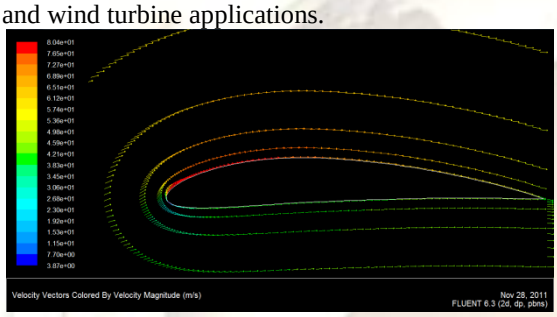

Fig 4: Velocity contours around NACA 4415 Airfoil at AOA=0^0

Figure 4 shows the velocity contours around the NACA 4415 foil. As can be seen the hump portion is fairly long with gradual rise in thickness giving a fairly uniform velocity level over much of the forward part of the airfoil.

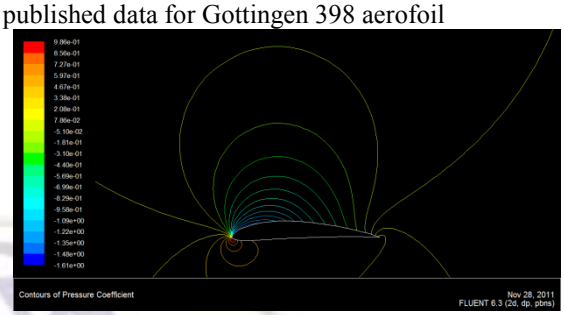

Fig 5: Pressure contours around NACA 4415 Airfoil at AOA=0^0

Figure 5 depicts the pressure contours enveloping the NACA 4415 airfoil. The low pressure area above the hump is also rather stretched out in keeping with the profile of the airfoil.

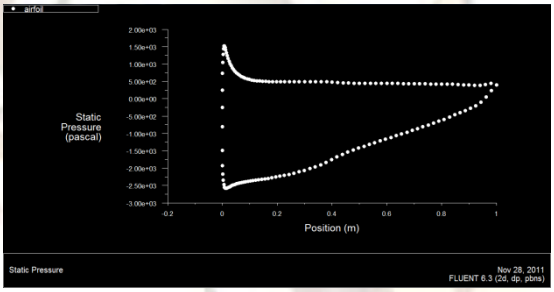

Fig 6: Pressure Coefficient along the chord line for NACA 4415 Airfoil at AOA=0^0

Figure 6 shows the chord wise pressure distribution over the upper and lower surfaces of the NACA 4415 airfoil. The fairly uniform (almost straight line) pressure curve of the upper surface correlates with the findings of the pressure distribution contours depicted in fig 5.

Force vector: (1 0 0)

zone name	pressure force n	viscous force n	total force n	pressure coefficient	viscous coefficient	total coefficient
airfoil	-160.88613	0	-160.88613	-0.10506733	0	-0.10506733
net	-160.88613	0	-160.88613	-0.10506733	0	-0.10506733

Force vector: (0 1 0)

zone name	pressure force n	viscous force n	total force n	pressure coefficient	viscous coefficient	total coefficient
airfoil	1890.4287	0	1890.4287	1.2345519	0	1.2345519
net	1890.4287	0	1890.4287	1.2345519	0	1.2345519

Table 3: Force reports of NACA 4415 Airfoil at AOA=2^0

ANGLE OF ATTACK	CFD DATA		PUBLISHED DATA		DIFF. CFD & PUBLISHED DATA	
	CL	Cd	CL	Cd	CL	Cd
0	0.369	0.0103	0.50	0.0080	-26.20%	28.75%

2	0.435	0.0125	0.65	0.0100	-33.08%	25.00%
4	0.760	0.0187	0.80	0.0200	-5.00%	-6.50%
6	0.931	0.0277	1.00	0.0300	-6.90%	-7.67%
8	1.118	0.0335	1.20	0.0350	-6.83%	-4.29%
10	1.195	0.0414	1.30	0.0400	-8.08%	3.50%
12	1.297	0.0505	1.40	0.0500	-7.36%	1.00%
14	1.378	0.0865	1.42	0.1000	-2.96%	-13.50%

Table: 4. Comparison of CFD data with NACA's published data for NACA 4415 aerofoil

Table 3 shown above is the force report for NACA 4415 generated by fluent software. Since NACA 4415 is a relatively thin airfoil expectedly it gives lower values of C_D as compared to Gottingen 398 as the wave drag in this case would be lower. However this advantage is counter set by the low values of C_L achieved at the matching AOA.

Table 4 enlists the C_L and C_D values of NACA 4415 Airfoil at various angles of attack as derived by CFD and compares them with NACA published values for that airfoil.

GOTTINGEN 535

This NACA airfoil was also developed in mid 50`s and has found lot of applications in aviation industry due to its high lift characteristics.

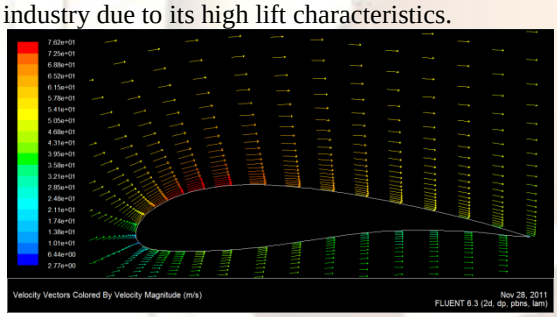

Fig 7: Velocity contours around Gottingen 535 Airfoil at AOA=0^0

Figure 7 shows the velocity contours that develop around the Gottingen 535 foil. This Velocity profile is characterised by very low values of velocity vector towards the rear end of the lower surface.

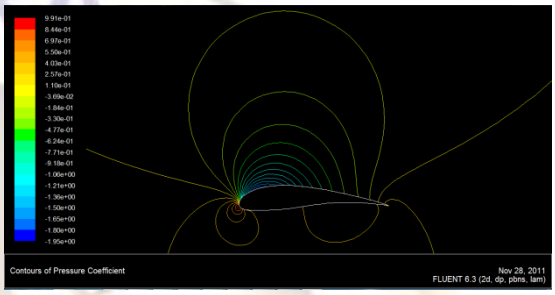

Fig 8: Pressure contours around Gottingen 535 Airfoil at AOA=0^0

Figure 8 depicts the pressure contours enveloping the Gottingen 535 airfoil.

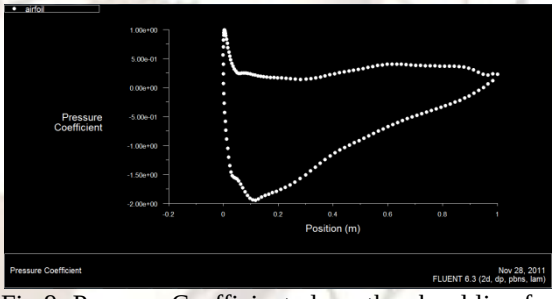

Fig 9: Pressure Coefficient along the chord line for Gottingen 535 Airfoil at AOA=0^0

Figure 9 shows the chord wise pressure distribution over the upper and lower surfaces of the Gottingen 535 airfoil. The prominently seen hump towards the left hand side of the upper curve corresponds to the high pressure region developed in the upwardly curving rear side of the lower surface.

Force vector: (1 0 0)

zone name	pressure force n	viscous force n	total force n	pressure coefficient	viscous coefficient	total coefficient
airfoil	-102.61826	0.97468468	-101.64358	-0.082737227	0.00078585144	-0.081951375
net	-102.61826	0.97468468	-101.64358	-0.082737227	0.00078585144	-0.081951375

Force vector: (0 1 0)

zone name	pressure force n	viscous force n	total force n	pressure coefficient	viscous coefficient	total coefficient
airfoil	1535.9786	0.036618688	1536.0152	1.2384015	2.9524265e-05	1.238431
net	1535.9786	0.036618688	1536.0152	1.2384015	2.9524265e-05	1.238431

Table 5: Force reports of Gottingen 535 Airfoil at AOA=0^0

ANGLE OF ATTACK	CFD DATA		PUBLISHED DATA		DIFF. CFD & PUBLISHED DATA	
	CL	Cd	CL	Cd	CL	Cd
0	0.674	0.0163	0.750	0.0110	-10.13%	48.18%
2	0.820	0.0187	0.960	0.0125	-14.59%	49.60%
4	1.007	0.0205	1.230	0.0150	-18.13%	36.67%
6	1.190	0.0212	1.450	0.0175	-17.93%	21.14%
8	1.298	0.0246	1.620	0.0200	-19.88%	23.00%
10	1.524	0.0278	1.780	0.0270	-14.38%	2.96%
12	1.767	0.0332	1.900	0.0375	-7.00%	-11.47%
14	1.828	0.0421	1.980	0.0570	-7.68%	-26.14%

Table:6. Comparison of CFD data with NACA's published data for GOTTINGEN 535 aerofoil

Table 5 shown above is the force report generated by fluent software. As mentioned earlier force vector (1,0,0) corresponds to the drag force experienced by the airfoil where as the vector (0,1,0) depicts the value of lift.

The lift and drag coefficients of Gottingen 535 airfoils for the angle of attack between 0 to 14 degrees at an interval of 2 degrees and the corresponding value is stated by NACA are tabulated in table 6.

As can be observed from the foregoing tables for the three NACA foils under investigation the variation between the values computed by numerical analysis and the values of lift and drag coefficient as published by NACA ranges from 2% to 25% with some exceptions. These variations can be attributed to certain assumptions made while doing the numerical analysis. Firstly the flow has been assumed to be Laminar under all circumstances. This is not true in reality. The NACA published data is largely based on large number of experiments which have been carried out by them at various facilities from time to time. Also the published data is not an outcome of just one experiment under one set of conditions but, a statistical average of various experimental results obtained under different conditions using different equipment over a period of time. Thus a certain amount of variation with the CFD results which have been obtained giving a single set of conditions to the solver can only be expected. The difference between the computed values and published values can also be attributed to the difference in Reynolds number. The values published by NACA correspond to a Reynolds number of 3 x 10^6, whereas the Reynolds number assumed for numerical solution by CFD is about 0.96 x 10^6. It may be observed that the values of C_d especially at higher angles of attack are markedly lower in CFD results than in actual experiments. This is owing to the inability of the numerical method to predict and account for flow separation that occurs towards the down stream end on the upper surface of the aerofoil.

Currently CFD is generally considered reliable only for flight regimes near cruise conditions were there is little or no separated flows and the deviations of the order of 10 to 30% are considered as reasonable[2, 9, 10].

Thus the present results being in reasonable agreement with each other for all practical purpose the CFD results and the methodology adopted as well as the boundary conditions employed may be treated as valid.

HLF Airfoil

Unlike the previously considered airfoils which have been developed to be used as wings or blades, the HLF airfoil has been developed with the objective of deploying it as a fuselage of an aircraft. This entails a trade off between various conflicting requirements; firstly the thickness has to be adequate to create enough cubical volume within the contours of the airfoil to accommodate the desired passenger and cargo capacities. Also the aerodynamic essentials viz: maximum lift and minimum drag have to be strived for along with ergonomic and architectural requirements. The provision for accommodating flight deck as well as avionics and control systems has also to be made. The airfoil so developed meeting the conflicting requirements has been designated as HLF(High Lift Generating Fuselage) aerofoil. This high lift generating airfoil was numerically analysed in a similar way as described earlier in case of other airfoils.

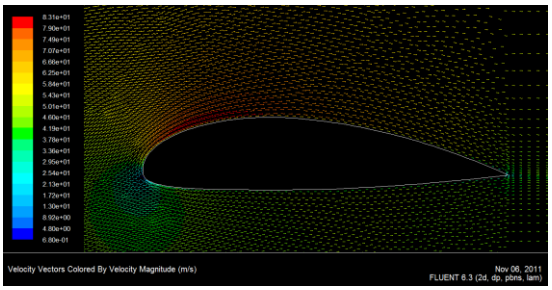

Fig 10: Velocity contours around HLF Airfoil at AOA=0^0

Figure 10 shows the velocity contours that develop around the HLF airfoil. As can be seen the velocities over the hump portion of the airfoil are substantially higher than those on the lower surface with maximum values exceeding those at the lower surface by a factor as high as 2.0.

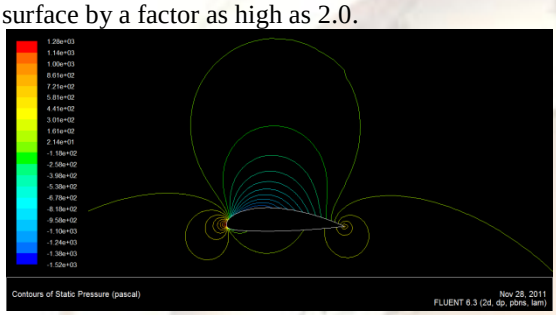

Fig 11: Pressure contours around HLF Airfoil at AOA=0^0

Figure 11 depicts the pressure contours enveloping the HLF airfoil. Predictably the low pressure areas above the hump coincide with the high velocity areas observed in figure 11 but the pressure contours are much gradual in nature in keeping with smoothness of the contours.

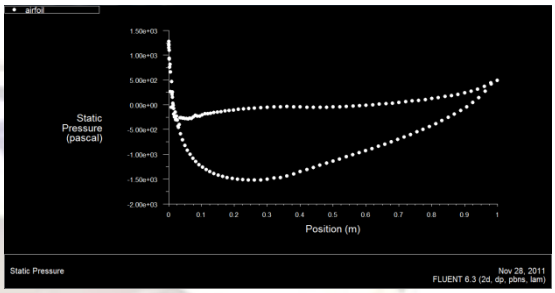

Fig 12: Pressure Coefficient along the chord line for HLF Airfoil at AOA=0^0

Figure 12 shows the chord wise pressure distribution over the upper and lower surfaces of the HLF airfoil. The uniform high pressure over the lower surface and significantly steep but smooth pressure gradient over the upper surface explains the high lift generated by this airfoil.

Force vector: (1 0 0)

zone name	pressure force n	viscous force n	total force n	pressure coefficient	viscous coefficient	total coefficient
airfoil	1.742416	0.33591892	2.0783349	0.0014048201	0.0002708341	0.0016756542
net	1.742416	0.33591892	2.0783349	0.0014048201	0.0002708341	0.0016756542

Force vector: (0 1 0)

zone name	pressure force n	viscous force n	total force n	pressure coefficient	viscous coefficient	total coefficient
airfoil	877.75429	0.0017380037	877.75603	0.70768801	1.4012627e-06	0.70768941
net	877.75429	0.0017380037	877.75603	0.70768801	1.4012627e-06	0.70768941

Table 7: Force reports of HLF Airfoil at AOA=0^0

ANGLE OF ATTACK	CFD DATA	
	CL	Cd
0	0.70761	0.00167868
2	0.9587	0.0023499
4	1.2054	0.0033566
6	1.4521	0.0044298
8	1.6708	0.0067398
10	1.9035	0.006779
12	2.107	0.0082801
14	2.2762	0.010381

Table:8. Tabulation of lift and drag coefficients of HLF aerofoil for various angles of attack.

Table 7 shown above is the force report of the HLF airfoil. The high values of lift with low values of drag can be conspicuously observed from the force report.

Table 8 above shows the values of C_L and C_D of HLF airfoil at various angles of attack as derived through CFD approach.

The comparative findings of the lift and drag characteristics of all the four airfoils viz: Gottingen 398, NACA 4415, Gottingen 535 and specially developed HLF airfoil, at various angles of attack, as found by numerical method have been graphically demonstrated in figures 13 & 14 respectively.

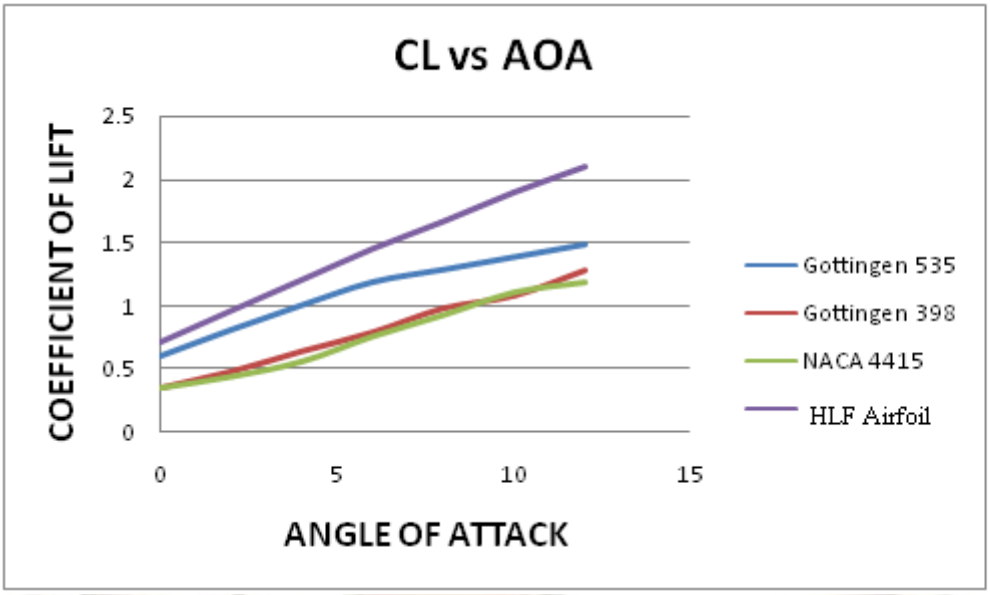

Fig13: The graph depicting Lift coefficient vs AOA for the four aerofoils investigated

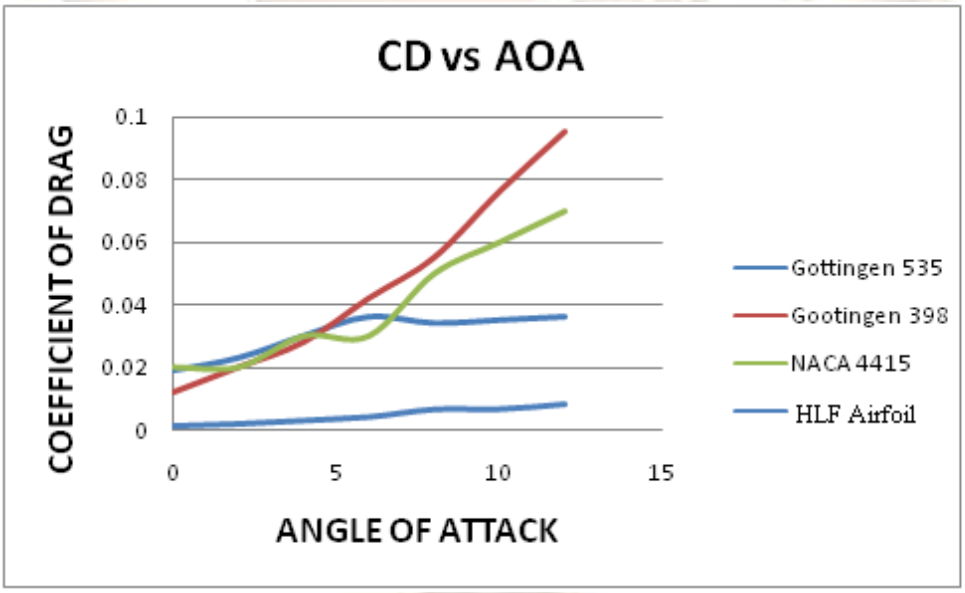

Fig 14: The graph depicting Drag coefficient vs AOA for the four aerofoils investigated.

DISCUSSION

The graphs above show the well established trend that the lift and the drag coefficients increase with the angle of attack [14, 15]. Since the curves for both NACA as well as HLF airfoil show continuous increase and no dropping in values of C_L it can be stated with certainty that the critical value of AOA is beyond 12 degrees which is the limit up to which the experimental work has been done in this case. This can be justified by the fact that the airfoil shapes are being investigated for fuselage application and so inclination beyond this would be impractical. Thus the stalling

phenomenon which gives rise to reduction in C_L and dramatic rise in C_D is not observed in these graphs.

It is also obvious from the results obtained that the HLF aerofoil has superior characteristics in terms

of the lift and the drag coefficients especially at lower angles of attack.

This unique advantage is also evidenced and can be attributed to the smooth velocity contours observed in the velocity profile depicted in figure 10 which shows significant gradients in velocity values without any flow separation. The smooth pressure contours and chord wise pressure distribution curves also explain the superiority of the aerodynamics of the airfoil and hence its performance. This is natural as the aerofoil has been specially developed for the application.

CONCLUSION

It is obvious from the foregoing results that the HLF aerofoil has much superior lift characteristics coupled with low drag characteristics especially at lower angles of attack. Quantitatively, in cruise conditions i;e at zero degrees AOA the Lift coefficient of HLF airfoil is higher by 57% than Gottingen 398, 91% than NACA 4415 and 4.9% than Gottingen 535, all of which are generically high lift generating airfoils. Also its C_D values are lower by 89% than Gottingen 398, 83% than NACA 4415 and 89% than Gottingen 535.

Further it is worth to mention that the HLF airfoil does not show any flow separation in the investigated range of AOA i;e from 0^0 to 12^0 and does not give rise to any stalling condition in this range of AOA.

This means that the proposed high lift generating HLF aerofoil is extremely suitable for deployment as an aircraft fuselage. Its rather large and uniform thickness over the significant portion of the chord imparts much sought cubical space within the contour of the airfoil. This makes it the ideal choice for the fuselage application to achieve short landing and takeoff (STOL) capabilities of aircraft.

REFERENCES

[1] Davis, W. R., Kosicki, B. B., Boroson, D. M., and Kostishack, Micro Air Vehicles for Optical Surveillance, *The Lincoln Laboratory Journal, Vol. 9, No. 2*, 1996, pp. 197-213.

[2] McGowan, A. R., AVST Morphing Project, Research Summaries in Fiscal Year 2001, *NASA TM 2002-211769*, August 2002.

[3] Mueller, T. J., (editor), *Conference on Fixed, Flapping and Rotary Wing Vehicles at Low Reynolds Numbers*, Notre Dame University, Indiana, June 5-7, 2000.

[4] Nathan Logsdon, Dr. Gary Solbrekken, *A Procedure For Numerically Analyzing Airfoils And Wing Sections*, doctoral diss., University of Missouri – Columbia, December 2006.

[5] F. X. Wortmann, The Quest for High Lift , *AIAA Paper 74-1018*, MIT- Cambridge, Sept. 1974.

[6] F. Le Chuiton, A. D.Alascio et al, *Computation of the Helicopter Fuselage Wake with the SST, SAS, DES and XLES Models*, Springer eBook, January 24, 2008.

[7] S. Melber-Wilkending, R. Rudnik et al, *Verification of MEGAFLOW Software for High Lift Applications*, Springer eBook, October 2, 2006.

[8] Christopher L. Rumsey, Susan X. Ying, Prediction of High Lift : review of present CFD capability, *Elsevier, Progress in Aerospace Sciences, volume 38, issue 2, February 2002.*

[9] Nicholas. K. Borer, Design and Analysis Of Low Reynolds Number Airfoil, *Project report MATH 6514 Industrial Math, 4 December 2002*.

[10] Alimul Rajib, Bhuiyan ,Shameem Mahmud etal, DESIGN ANALYSIS OF UAV (UNMANNED AIR VEHICLE) USING NACA 0012 AEROFOIL PROFILE. .